

A Combined Control Strategy for Load Management within an Interconnected Nanogrid Network

Daniel Burmester Ramesh Rayudu Winston K.G. Seah
School of Engineering and Computer Science
Victoria University of Wellington
PO Box 600, Wellington 6140, New Zealand
{Daniel.Burmester,Ramesh.Rayudu,Winston.Seah}@ecs.vuw.ac.nz

Abstract—The financial viability of small scale household photovoltaic systems is increasing due to advances in efficiency and reduction in price. However, one of the major issues is the intermittent nature of photovoltaic installations. Researchers are now pursuing new power topologies and control techniques to address this issue. In this paper, an interconnected nanogrid control scheme is presented, using thermostatically controlled loads over traditional storage techniques. When comparing the controlled system to an uncontrolled system, it was found that the grid power consumed by the interconnected nanogrid network was reduced by as much as 55%.

I. INTRODUCTION

One of the major issues deterring the uptake of household photovoltaic installations is intermittency [1]. This consists of fluctuations in power production throughout the day (due to environmental events e.g. cloud cover) and a lack of power production during the night. In light of such issues, researchers are investigating new power topologies and control techniques to reduce the impact of intermittency.

One such solution is a nanogrid which is considered a bottom up approach to power systems due to its modular nature [2]. Their flexibility can facilitate the creation of larger power entities such as microgrids, or “Interconnected nanogrid networks” [3].

Interconnected nanogrid networks are discussed mostly at a conceptual level within the literature [1], [2], [4]. However, the research presented in [3], [5], [6] take it further with an in-depth analysis and testbed presented. While these papers serve as a knowledge base for interconnected nanogrid networks, there is little in the way of control discussed within the literature. This paper presents a combined control scheme comprising of interconnected nanogrid controllers creating a comprehensive control strategy.

II. NANOGRID SYSTEM

In the context of this research, a nanogrid is a DC power distribution system for a single house/small building, with the ability to connect or disconnect from the national grid. It consists of local PV power production, powering local loads

978-1-5386-4950-3/17/\$31.00 ©2017 IEEE

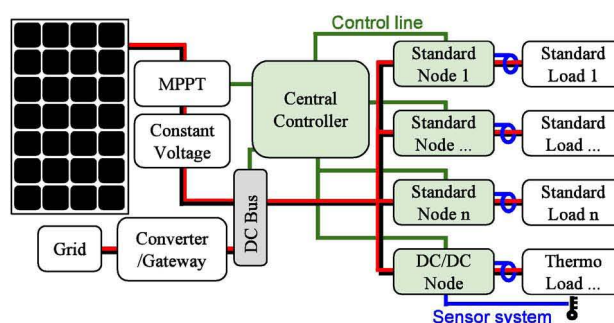


Fig. 1: Block diagram of the nanogrid control topology [9]

and control systems to increase the nanogrid’s operational efficiency [1]. DC power is selected due to the increased efficiency it can deliver as a result of fewer power conversions in [7].

The control topology selected for this system is hybrid central control as outlined in [8]. It consists of a central controller with the ability to communicate with decentralised control nodes as displayed in Fig. 1.

While the central controller undertakes a coordinating role within the control strategy, facilitating interactions between the maximum power point tracker (MPPT) and decentralised nodes, the nodes implement real-time control. As described in [9], the MPPT not only implements its traditional purpose of maximising the power output of the photovoltaics (PV), the MPPT’s algorithm is also used by the control scheme to observe the available PV power at any particular time. This gives real-time information about the local production regardless of the households consumption. The nanogrid control scheme can then use this data to make informed decisions about where to best allocate the available power.

The control nodes have the ability to sense the current and voltage consumed by any load within the nanogrid, as well as sensing the temperature output of the TCLs. While the “standard” nodes shown in Fig. 1 can switch loads on/off depending on the status required by the nanogrid control scheme, the “DC/DC” nodes are equipped with a buck converter, allowing

TABLE I: Explanation of variables in Eqn. (1) and (2)

Variable	Description	Simulation Values
M	Mass of water (kg)	88L to 300L
c	Specific heat of the water ($J/kg^{\circ}C$)	4179 $J/kg^{\circ}C$
\dot{m}	Flow rate (kg/h)	9L/m
T_W	Temperature of the water in the tank ($^{\circ}C$)	55 $^{\circ}C$ to 81 $^{\circ}C$
T_i	Temperature of the water entering the tank ($^{\circ}C$)	7 $^{\circ}C$
h	Heat transfer coefficient (for convection to ambient) ($W/m^2^{\circ}C$)	1.5W/ $m^2^{\circ}C$
A	Area of the tank (m^2)	1.84 m^2 to 3.85 m^2
T_a	Ambient temperature ($^{\circ}C$)	20 $^{\circ}C$
q	Heat rate of the heating element (W)	2kW to 3kW
t	time (s)	

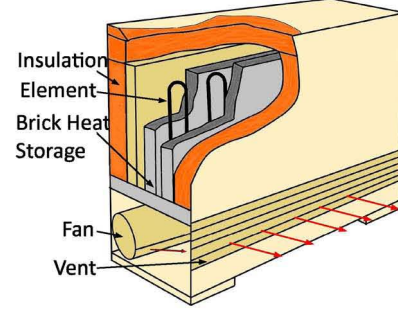


Fig. 2: Storage Heater Diagram [9]

the control scheme to vary the applied voltage.

III. THERMOSTATICALLY CONTROLLED LOADS

A Thermostatically Controlled Load (TCL) is a load that has little to no input from the user, instead switching on/off when its temperature criteria is met. The nanogrid makes use of the TCL's relatively slow dynamics to store energy which can be used outside of PV production times. During the design of the nanogrid, two TCLs were identified as large consumers of power and selected for analysis and control. These were the electric water heater and space heating, of which the analysis and control theory are presented below.

A. Water Heater

A household water heater is responsible for supplying the residents with hot water for showers, sink use etc. It has an input of cold water (7 $^{\circ}C$) which it is required to heat and keep above 55 $^{\circ}C$ to avoid bacteria forming in the tank. Generally, the upper temperature limit for a water heater is around 65 $^{\circ}C$, however in this study we allow the water to heat to 81 $^{\circ}C$, increasing the thermal autonomy (time between "on" cycles), and apply a thermostatic mixing valve on the output to avoid scolding.

Eqn. (1) shows the differential equation that describes the behaviour of the water heater. This equation can be rearranged to calculate the time taken for the water to cool/heat from one temperature to another (eqn. (2)). The variables for each is explained in table I.

$$Mc \frac{dT_W}{dt} = \dot{m}c(T_i - T_W) - hA(T_W - T_a) + q \quad (1)$$

$$t = \frac{b \times \log(x)}{a + d} \quad (2)$$

where $x = \frac{k}{T_W - f}$ and $f = \frac{aT_i + dT_a + q}{a + d}$, with k being the integration constant, $a = \dot{m}c$, $b = Mc$ and $d = hA$.

B. Storage heater

The storage heater was selected for this project, as a means of space heating, due to its high thermal capacity. It is depicted in Fig. 2 where it can be seen that it consists of heating elements (much like that of the water heater), brick thermal

storage, and insulated housing and a fan. When power is applied, the elements heat the bricks, the stored heat can be extracted, via the fan, at the required time.

There are two modes of operation for the storage heater, fan on and fan off. The equations that describe the behaviour of both modes are displayed below, again rearranged to ensure on/off time can be calculated.

Fan off

$$M_b c_b \frac{dT_b}{dt} = Q_{In} - \frac{k_{fb} A_{fb}}{l_{fb}} \Delta T - \frac{k_s A_s}{l_s} \Delta T - k_{vn} A_{vn} \Delta T \quad (3)$$

where ΔT is temperature of the bricks (T_b) minus the temperature of the room (T_R). The variables can be taken from Table II.

$$t = \frac{\log(\frac{w}{T_b - p})}{a + b + c} \quad (4)$$

where $a = \frac{k_{fb} A_{fb}}{l_{fb} M_b c_b}$, $b = \frac{k_s A_s}{l_s M_b c_b}$, $c = \frac{k_{vn} A_{vn}}{M_b c_b}$,

$p = \frac{Q_{In} + (a + b + c)T_R}{a + b + c}$ and w is the constant of integration.

Fan on

$$M_b c_b \frac{dT_b}{dt} = -\frac{k_{fb} A_{fb}}{l_{fb}} \Delta T - \frac{k_s A_s}{l_s} \Delta T - k_{vf} A_{vf} \Delta T \quad (5)$$

where ΔT is temperature of the bricks (T_b) minus the temperature of the room (T_R). The variables in Eqn. (5) can be taken from Table II with the exception of k_{vf} which is the forced convection heat transfer coefficient, and A_{vf} is equal in area to A_{vn} .

$$t = \frac{\log(\frac{w}{T_b - T_R})}{a + b + d} \quad (6)$$

where $a = \frac{k_{fb} A_{fb}}{l_{fb} M_b c_b}$, $b = \frac{k_s A_s}{l_s M_b c_b}$, $d = \frac{k_{vf} A_{vf}}{M_b c_b}$ and w is the constant of integration.

Equations (1) to (6) are used within the combined control law to determine the power allocated to each load.

TABLE II: Explanation of variables in Eqn. (3) to (6)

Variable	Description	Simulation Values
M_b	Mass of the bricks (kg)	$60kg$
c_b	Specific heat of the bricks ($J/kg^\circ C$)	$670J/kg^\circ C$
T_b	Temperature of the bricks ($^\circ C$)	$20^\circ C$ to $600^\circ C$
k_{fb}	Thermal conductivity of front and back ($W/m^\circ C$)	$0.021W/m^\circ C$
A_{fb}	Area of the front and back (m^2)	$0.698m^2$
l_{fb}	Thickness of the front and back (m)	$0.009m$
k_s	Thermal conductivity of the sides/top/bottom ($W/m^\circ C$)	$0.04W/m^\circ C$
A_s	Area of the sides/top/bottom (m^2)	$0.345m^2$
l_s	Thickness of the sides/top/bottom (m)	$0.05m$
k_{vn}	Natural convection heat transfer coefficient ($W/m^2^\circ C$)	$10.45W/m^2^\circ C$
A_{vn}	Heat transfer area of the surface (m^2)	$0.034914m^2$

IV. COMBINED CONTROL NANOGRID NETWORK

A progression of the individually controlled nanogrid network presented in [9], the combined control nanogrid network expands the control strategy from multiple individual systems, to one larger network. The network can be thought of as a step up in the hierarchical structure of the nanogrid. Where the central controller was the top tier (in the individual nanogrid control strategy), now the interconnected nanogrid controller adopts this role. As the block diagram displayed in Fig. 3 indicates, the nanogrid's central controller still coordinates the node controllers, but now the interconnected nanogrid controller coordinates interactions between each of the nanogrids in the cluster. This means the control strategy is not only aware of the consumption and production of the individual houses, but of all the houses combined within the cluster.

To implement combined control law, the duty cycle (relating to the buck converter in the DC/DC node) calculated for each TCL must consider all other loads and supplies operating in the network. Equation (7) shows the maximum power point tracking supply signal for the nanogrid network. It is a summation of all the available PV power within the nanogrid network. Just as the nanogrid's loadline can be diverse, so can the PV capacity of each house.

$$P_{MPPT_{micro}} = P_{I_{n_{micro}}} = \sum_{i=1}^j V_{I_{n_i}} I_{I_{n_i}} \quad (7)$$

where j is the number of interconnected nanogrids, $P_{I_{n_{micro}}}$ is the PV power produced by each house while $V_{I_{n_i}}$ and $I_{I_{n_i}}$ refers to the voltage and current produced by each house respectively.

The power delivered to each of the nanogrid network's TCLs by the control law must also be calculated. Equations (8) through (11) show how the duty cycle (D) is calculated, as a function of current (I_{In} , I_o), for the buck converter present in the TCL's node. It considers the efficiency of the buck converter (\mathcal{E}), output/input power (P_o and P_{In} , respectively), and output/input voltage (V_o and V_{In} , respectively).

$$V_o = DV_{In} \quad (8)$$

$$P_o = \mathcal{E}P_{In} \quad (9)$$

$$DV_{In}I_o = \mathcal{E}V_{In}I_{In} \quad (10)$$

$$D = \frac{\mathcal{E}V_{In}I_{In}}{V_{In}I_o} = \frac{\mathcal{E}I_{In}}{I_o} \quad (11)$$

Equations (12) and (13) consider the new variable $P_{MPPT_{micro}}$ and also introduce $V_{I_{n_{micro}}}$, a summation of the voltages ($V_{I_{n_i}}$) produced by the combined PV installations. This is used to derive the current produced by the interconnected nanogrid network ($I_{I_{n_{micro}}}$). The duty cycle determining the output voltage of a TCL's control node can then become a function of the power generated by the nanogrid network (14).

$$V_{I_{n_{micro}}} = \frac{\sum_{i=1}^j V_{I_{n_i}}}{j} \quad (12)$$

$$I_{I_{n_{micro}}} = \frac{P_{MPPT_{micro}}}{V_{I_{n_{micro}}}} \quad (13)$$

$$D = \frac{\mathcal{E}P_{MPPT_{micro}}}{I_o V_{I_{n_{micro}}}} \quad (14)$$

Although equation (14) gives the duty cycle for the control node, it does not consider other loads operating within the

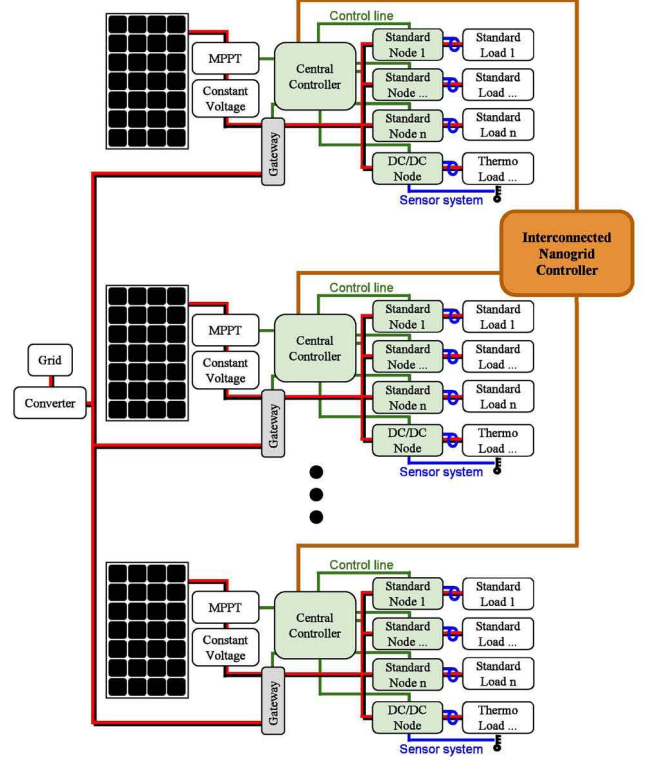


Fig. 3: Block diagram of the interconnected nanogrid topology with combined control

nanogrid network. The duty cycle will need to be adjusted to consider the uncontrolled and TCLs operating in the network.

To do so, equation (15) is used to calculate the consumption of all uncontrolled loads consuming power within the nanogrid network. These are loads that the consumer controls and expects an output when they are switched on. Such loads are not controlled within the nanogrid to ensure the comfort of the user.

$$L_{total_micro} = \sum_{m=1}^n L_{total_m} \quad (15)$$

where n is the number of loads operating, that are not thermostatically controlled.

Next the measure of urgency (defined here as the power consumption of a load in a day) of each TCL needs to be calculated. Equation (16) is used to calculate an estimated “on” time for each TCL based on its current temperature, usage and thermal characteristics. The premise of this calculation is that, the load that will consume the largest amount of power for a particular time period (day) is the most urgent and needs to be serviced by PV power. The variable x relates to a load being powered while x_1 is used if a load is not drawing power. For the water heater, equations (17) and (18) are used and the space heater, equations (19) and (20) (variables for water and storage heater equations explained in tables I and II respectively).

$$u_T = P \frac{\log(x)}{\log(x) + \log(x_1)} / \text{day} \quad (16)$$

for water heater:

$$x = \frac{k}{T_W - \frac{\dot{m}cT_i + hAT_a + q}{\dot{m}c + hA}} \quad (17)$$

where k is the constant of integration.

$$x_1 = \frac{k_1}{T_W - \frac{\dot{m}cT_i + hAT_a}{\dot{m}c + hA}} \quad (18)$$

where k_1 is the constant of integration.

for space heater:

$$x = \frac{w}{T_b - p} \quad (19)$$

where $p = \frac{Q_{In} + (a + b + c)T_R}{a + b + c}$, $a = \frac{k_{fb}A_{fb}}{l_{fb}M_b c_b}$, $b = \frac{k_s A_s}{l_s M_b c_b}$, $c = \frac{k_{vn} A_{vn}}{M_b c_b}$ and w is the constant of integration

$$x_1 = \frac{w_1}{T_b - T_R} \quad (20)$$

where w_1 is the constant of integration.

The measure of urgency is then converted to a ratio as shown in equation (21). This creates a hierarchy of the most to least urgent loads and gives a scaling factor for the duty cycle which is calculated in equation (22). This duty cycle is the signal

given to a control node, controlling load y , by the central controller, ensuring the load receives the ratio of available PV power that is allocated.

This means, within the nanogrid network, the loads that are likely to draw the largest quantity of power over a given period of time (day), will be serviced with the majority of the available PV power. It stands to reason that as a load receives power, heating its thermal mass, it's measure of urgency descends until the another load becomes more urgent and is turned on.

$$m_{micro_y} = \sum_{y=1}^z \frac{u_{T_y}}{\sum_{w=1}^z u_{T_w}} \quad (21)$$

where z is the number of TCLs within the cluster of houses

$$D_{ratio_y} = m_{micro_y} \frac{\mathcal{E}(P_{MPPT_micro} - L_{total_micro})}{I_{o_y} V_{In_micro}} \quad (22)$$

It is important to note the following safety measure which can override the control law.

- *Water Lower Temperature Threshold:* The water heater will be switched on, regardless of PV power availability, if a lower temperature threshold is reached.
- *Room Temperature:* Rooms will be kept at a specific temperature regardless of PV power availability.
- *Upper Temperature Limits* Both the water and storage heaters have upper temperature limits which will not be exceeded.

V. SIMULATION, RESULTS AND DISCUSSION

In order to quantify the technical success of the combined control nanogrid network, a controlled and uncontrolled nanogrid network was simulated in MATLAB's Simulink with the PLECS extension software. Test scenarios were then established considering winter and summer solar irradiance, as well as household power consumption curves, which vary with the seasons, in order to create realistic simulated test conditions.

Fig. 4 shows one week of summer and winter power output of a 6kW PV installation, with irradiance data from Kelburn, New Zealand (data taken from NIWA solar view) [10]. This was applied to the seven load curves shown in Fig. 5 (red is winter consumption, while blue is summer), which were used to create interconnected clusters of houses with the cluster sizes ranging from two to seven (a more in-depth description of the system is given in [9]). The grid power consumed by each of the clusters (two to seven houses), controlled and uncontrolled, was monitored the two scenarios were compared over the summer and winter weeks.

Fig. 6 shows the reduction in grid power consumed by the combined control nanogrid network when compared to the uncontrolled nanogrid network. It can be seen that in each case the controlled scenario outperformed the uncontrolled by a substantial amount (as a much as 55%). With the

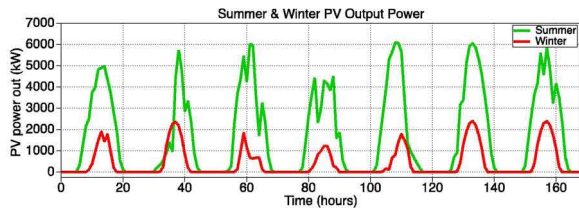


Fig. 4: PV output for summer and winter in Kelburn NZ [9]

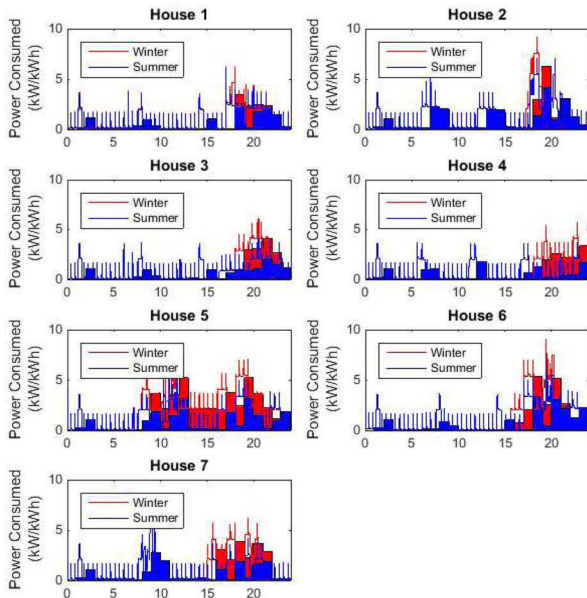


Fig. 5: Uncontrolled household consumption curves displayed in instantaneous (lines) and average power consumed during each hour of the day (blocks)

smaller clusters, 2 and 3 houses, the reduction 42% and 48% respectively, while the remaining houses were all within 2.5% of the highest reduction level (55%).

Fig. 7 shows a 24 hour period of the 7 house cluster controlled, and uncontrolled. It can be seen that in the controlled scenario, the cluster consumes the majority of available PV power, while the uncontrolled utilises very little.

VI. CONCLUSIONS

This paper present a combined control system for a nanogrid network which uses TCLs to increase PV power consumed and reduce power consumed from the grid by a small cluster of houses. The control system utilises the MPPT signal to observe PV production and alters the power draw of the TCLs to ensure all of the available PV power is being used, storing the energy in thermal form. The system can reduce grid consumption by as much as 55% given a 7 house scenario.

REFERENCES

[1] D. Burmester, R. Rayudu, W. K. G. Seah, and D. Akinyele, "A review of nanogrid topologies and technologies," *Renewable and Sustainable Energy Reviews*, vol. 67, pp. 760 – 775, 2017.

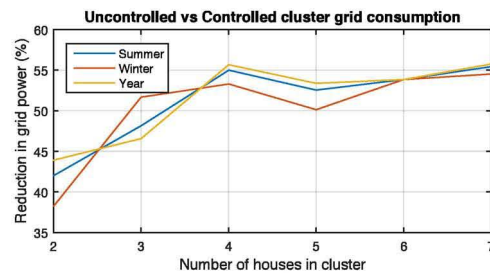


Fig. 6: Reduction in grid power consumed

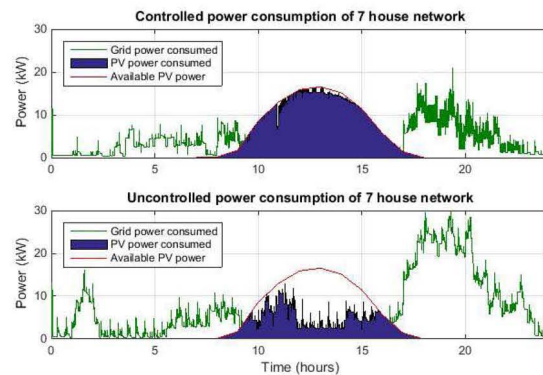


Fig. 7: Comparison of controlled and uncontrolled 7 house scenario over a 24 hour period in Winter

[2] B. Nordman and K. Christensen, "Local power distribution with nanogrids," in *2013 International Green Computing Conference Proceedings*, June 2013, pp. 1–8.

[3] A. Werth, N. Kitamura, I. Matsumoto, and K. Tanaka, "Evaluation of centralized and distributed microgrid topologies and comparison to open energy systems (oes)," in *2015 IEEE 15th International Conference on Environment and Electrical Engineering (EEEIC)*, June 2015, pp. 492–497.

[4] D. Boroyevich, I. Cvetković, D. Dong, R. Burgos, F. Wang, and F. Lee, "Future electronic power distribution systems a contemplative view," in *2010 12th International Conference on Optimization of Electrical and Electronic Equipment*, May 2010, pp. 1369–1380.

[5] A. Werth, N. Kitamura, and K. Tanaka, "Conceptual study for open energy systems: Distributed energy network using interconnected dc nanogrids," *IEEE Transactions on Smart Grid*, vol. 6, no. 4, pp. 1621–1630, July 2015.

[6] A. Werth, M. Tokoro, and K. Tanaka, "Bottom-up and recursive interconnection for multi-layer dc microgrids," in *2016 IEEE 16th International Conference on Environment and Electrical Engineering (EEEIC)*, June 2016, pp. 1–6.

[7] K. Johnson, V. Vossos, M. Kloss, G. Robinson, and R. Brown, "Direct current as an integrating platform for zne buildings with evs and storage: Dc direct systems—a bridge to," 2016.

[8] J. K. Schönberger, "Distributed Control of a Nanogrid Using DC Bus Signalling," Ph.D. dissertation, University of Canterbury, Christchurch, New Zealand, May 2005.

[9] D. Burmester, R. Rayudu, and W. K. G. Seah, "Use of maximum power point tracking signal for instantaneous management of thermostatically controlled loads in a dc nanogrid," *IEEE Transactions on Smart Grid*, vol. PP, no. 99, pp. 1–1, 2017.

[10] National Institute of Water and Atmospheric research. Niwa solar view. [Online]. Available: <http://solarview.niwa.co.nz>